

Unsupervised brain lesion segmentation from MRI using a convolutional autoencoder

Hans E. Atlason^{*a}, Askell Love^{b,c}, Sigurdur Sigurdsson^d, Vilmundur Gudnason^{b,d}, and Lotta M. Ellingsen^{a,e}

^aDept. of Electrical and Computer Engineering, University of Iceland, Reykjavik, Iceland

^bDept. of Medicine, University of Iceland, Reykjavik, Iceland

^cDept. of Radiology, Landspítali - University Hospital, Reykjavik, Iceland

^dThe Icelandic Heart Association, Kopavogur, Iceland

^eDept. of Electrical and Computer Engineering, The Johns Hopkins University, Baltimore, MD, USA

ABSTRACT

Lesions that appear hyperintense in both Fluid Attenuated Inversion Recovery (FLAIR) and T2-weighted magnetic resonance images (MRIs) of the human brain are common in the brains of the elderly population and may be caused by ischemia or demyelination. Lesions are biomarkers for various neurodegenerative diseases, making accurate quantification of them important for both disease diagnosis and progression. Automatic lesion detection using supervised learning requires manually annotated images, which can often be impractical to acquire. Unsupervised lesion detection, on the other hand, does not require any manual delineation; however, these methods can be challenging to construct due to the variability in lesion load, placement of lesions, and voxel intensities. Here we present a novel approach to address this problem using a convolutional autoencoder, which learns to segment brain lesions as well as the white matter, gray matter, and cerebrospinal fluid by reconstructing FLAIR images as conical combinations of softmax layer outputs generated from the corresponding T1, T2, and FLAIR images. Some of the advantages of this model are that it accurately learns to segment lesions regardless of lesion load, and it can be used to quickly and robustly segment new images that were not in the training set. Comparisons with state-of-the-art segmentation methods evaluated on ground truth manual labels indicate that the proposed method works well for generating accurate lesion segmentations without the need for manual annotations.

Keywords: MRI, brain, segmentation, white matter lesions, autoencoder

1. INTRODUCTION

Lesions that correspond to white matter (WM) hyperintensities in Fluid Attenuated Inversion Recovery (FLAIR) and T2-weighted (T2-w) magnetic resonance images (MRIs) have been shown to be positively associated with age and neurodegenerative diseases.¹ Such lesions are observed in 96% of volunteers over the age of 65.¹ An accurate segmentation of these lesions is important in large-scale imaging studies of the elderly, both because the lesions are important biomarkers to characterize brain diseases and because they can interfere with the segmentation of other brain structures if not accounted for in automated segmentation approaches. The currently accepted gold standard in lesion segmentation is manual delineation by an expert in neuroanatomy. However, acquiring such delineations is both time consuming and expensive and studies have shown that human raters can have great intra- and inter-rater variability.²

Multiple automatic lesion segmentation methods have been developed that can be categorized into supervised and unsupervised methods. Supervised methods rely on training sets that consist of MRIs and corresponding manually delineated lesions. Although supervised methods with convolutional neural networks (CNNs) have shown to achieve state-of-the-art performance on various data sets,²⁻⁴ manual delineations often don't exist when analyzing new data sets and creating them may not be practical. Unsupervised methods typically involve modeling of MRI brain tissue intensities. This can be challenging because tissue intensities of MRIs are not always consistent within an image (e.g., due to inhomogeneity artifacts) or between different images (e.g., due to

scanner differences). Artifacts or poor skull-stripping can lead to high-intensity regions in FLAIR images that could potentially be incorrectly classified as lesions. Furthermore, the number of lesions and their location is unknown beforehand and can vary greatly between subjects, with some subjects having no lesions while others have an abundance of them. When using such automated approaches to process large data sets of brain MRIs, one must be able to trust that lesion boundaries are consistent within and across subjects, and that the methods are reliable and robust to different sizes and numbers of lesions.

Various methods have been proposed for unsupervised lesion segmentation, e.g. methods that use tissue segmentation to obtain lesions^{5,6} (usually as outliers of tissue⁷), and approaches that use only specific lesion properties.^{7,8} Furthermore, lesions can be detected as outliers of pseudo-healthy synthesized images,^{9,10} however, a necessary requirement for these approaches to work is to have a training data set with healthy brains to model normality, such that lesions can be detected either as outliers or as results of large reconstruction errors.⁹⁻¹¹ This is not the case when analyzing data sets of elderly subjects, where the variability in lesion load (both number and size of lesions) can be extremely high. The proposed method addresses this problem, by enabling unsupervised tissue and lesion classification with a convolutional autoencoder without the need to model lesions as anomalies in the brain. We propose to model the intensities of FLAIR images as a conical combination of the segmentation of WM, gray matter (GM), cerebrospinal fluid (CSF), and lesions, estimated by a convolutional autoencoder from the corresponding T1, T2 and FLAIR images. Some of the advantages of this model are that it accurately learns to segment lesions regardless of lesion load, and it can be used to quickly and robustly segment new images that were not in the training set. We will hereafter refer to the proposed method as the Segmentation Auto-Encoder (SegAE).

2. METHOD

2.1 Data and preprocessing

The AGES-Reykjavik Study¹² cohort comprises 5764 participants (female and male, age 66-93), 4811 of which underwent brain MRI. The MRIs were acquired using a dedicated General Electrics 1.5-Tesla Signa Twinspeed EXCITE system with a multi-channel phased array head cap coil. T1-weighted (T1-w) images (TE = 8 ms, TR = 21 ms) with $0.94 \times 0.94 \times 1.5$ mm³ voxel size; T2-w fast spin echo sequence (TE = 90 ms, TR = 3220 ms); and FLAIR sequence (TE = 100ms, TR = 8000ms) with $0.86 \times 0.86 \times 3.0$ mm³ voxel size.

For developmental purposes, we randomly selected 50 subjects from the AGES-Reykjavik study; 30 subjects for training, 5 for validation of model parameters, and 15 for testing. The WM lesions in the test images were manually annotated by an experienced neuroradiologist. The images used for validation were used to determine model architecture and hyperparameters based on visual inspection.

The images were preprocessed using standard preprocessing procedures: Resampling to $0.8 \times 0.8 \times 0.8$ mm³ voxel size, correction for signal non-uniformity¹³ in the T1-w and T2-w images (see subsection 2.3 for why FLAIR was omitted), rigid registration to the MNI-ICBM152 template,¹⁴ and skull removal.¹⁵

2.2 Network architecture and training procedure

The proposed method, SegAE, makes use of an autoencoder with fully convolutional layers on three resolution scales. The input to SegAE consists of three-dimensional (3D) patches of size $80 \times 80 \times 80$ voxels each, from T1-w, T2-w, and FLAIR images. The autoencoder is then trained to minimize the loss L:

$$L = (Y^p - \hat{Y}^p)^2,$$

where Y is a FLAIR patch, \hat{Y} is the corresponding reconstructed FLAIR patch from the autoencoder, and $p = 3$ to give more weight to the hyperintense lesions. A brainmask¹⁵ is applied before the loss so the background is not considered. The last layer is a one-by-one convolution constrained to have positive weights and no bias.¹⁶ The input to the last layer has a sum-to-one constraint enforced with a softmax activation function. This is an ill-posed problem, so regularization is needed. We want to push the sum-to-one layer to generate binary segmentations. This is done by constraining the input to the softmax function to be in a certain range (0-200) along the channel axis.

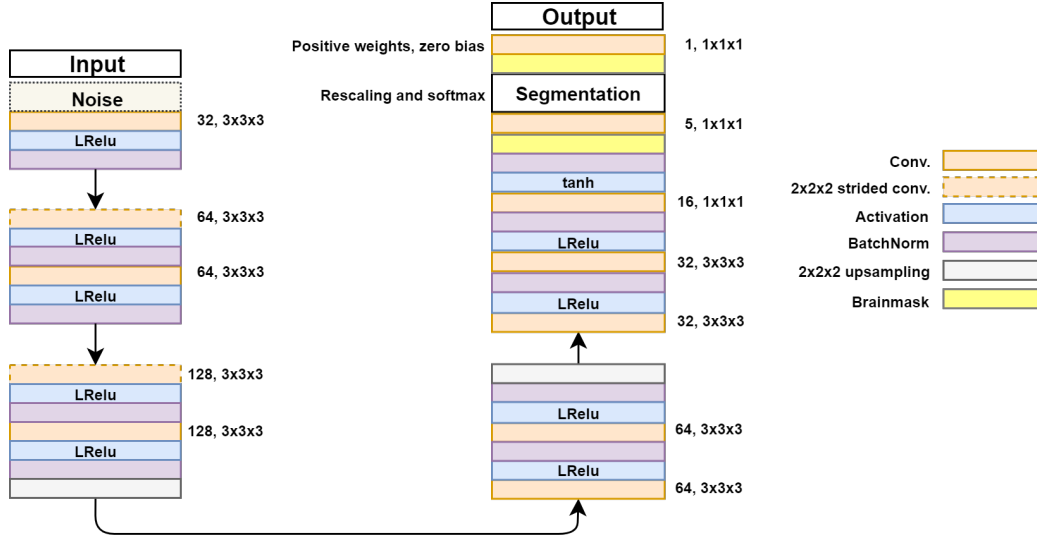


Figure 1. The proposed convolutional autoencoder architecture. The input is 3D patches from T1, T2, and FLAIR MRIs. The number of filters and kernel size are shown next to the corresponding convolutional layers. The Segmentation layer denotes a rescaling of the activations and an application of a softmax function. The final convolutional layer is restricted to have positive weights and zero bias for the output reconstruction of the FLAIR patch to be a conical combination of the Segmentation layer.

Patches were normalized to have unit mean WM before training, using a WM segmentation mask. We used FreeSurfer¹⁷ to generate this mask, however, any tissue segmentation method can be used. To make the network less sensitive to image normalization the training patches of each channel were multiplied by a constant drawn from a Gaussian distribution with a mean value of 1.0 and standard deviation of 0.5 during training. Furthermore, Gaussian noise with zero mean and a standard deviation of 0.05 was added to the input during training for noise robustness. The network architecture for the convolutional autoencoder can be seen in Figure 1. Patches from the 30 training images were acquired with a stride of 40, and a GTX1080 Ti GPU was used to train the network for 50 epochs with a learning rate of 0.001 using the Adam optimizer¹⁸ with $\beta_1 = 0.99$ and $\beta_2 = 0.99999$ and a batch size of one. Leaky rectified linear unit (LReLU) activation functions had a slope of 0.1 for the negative part. Hyperparameters were chosen by trial and error.

2.3 Prediction and post-processing

After training, one of the five Segmentation output volumes (see Figure 1) that corresponds to lesion segmentation was used for prediction, and other outputs were discarded. Prediction was performed with a stride of 20, and patches were assembled using the average of overlapping voxels. A threshold of 0.5 was used to binarize the average predictions. Initially, N4¹³ was used for inhomogeneity correction in the T1, T2 and FLAIR images. However, we observed that FLAIR lesions tended to degrade after N4 correction. Therefore, we did not use N4 correction on the FLAIR images used for training and testing SegAE, resulting in some high intensity inhomogeneity artifacts appearing mainly in the anterior and posterior parts of the cortical gray matter.

Following the autoencoder, an additional post-processing step was included involving multiplying the result from SegAE with two morphologically eroded brainmasks. The first brainmask was obtained by morphologically eroding the skullstripping mask with a 3x3x3 cube in 10 iterations. The second brainmask was obtained from FreeSurfer (binarized segmentation excluding sulcal CSF) and morphologically eroded with a 3x3x3 cube in 2 iterations. The post-processing removed most of the inhomogeneity artifacts from the validation subjects, as well as artifacts due to failures in skullstripping. Although we used FreeSurfer to generate the brainmask that excludes sulcal CSF, any algorithm capable of producing such a brainmask would work.

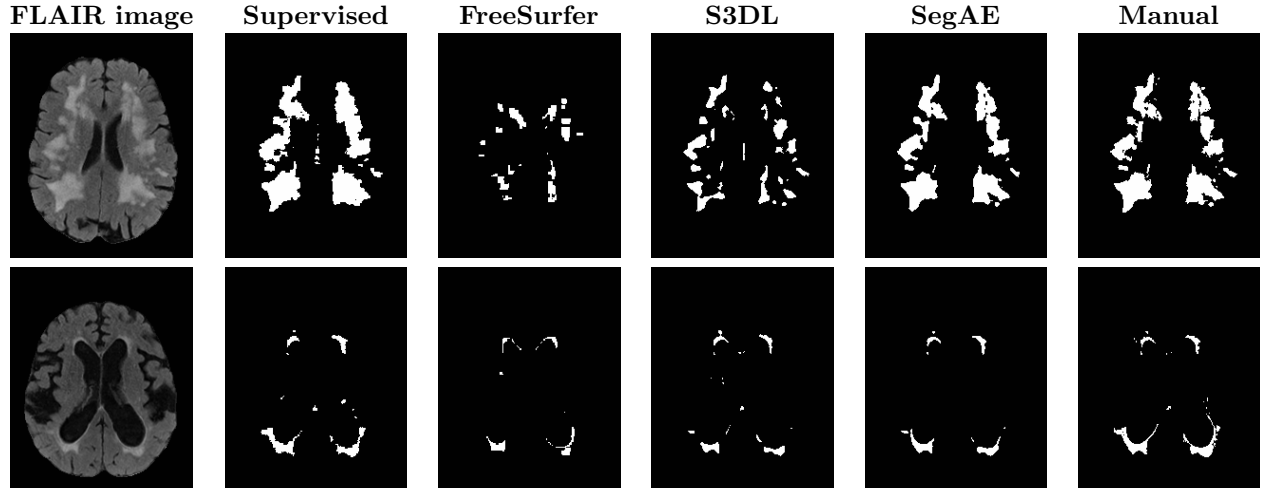


Figure 2. Visual comparison of the proposed method and three state-of-the-art methods with a manual rater for two different subjects, one with a high lesion load (top row) and one with a smaller lesion load but with enlarged ventricles (bottom row).

3. RESULTS AND DISCUSSION

The white matter lesions in a total of 15 subjects were manually delineated by a neuroradiologist to be used as ground truth lesion segmentations for evaluation of the proposed method. We compared the proposed method with three state-of-the-art segmentation methods: 1) A supervised tissue segmentation developed for the AGES-Reykjavik data set, created with an artificial neural network classifier in the four dimensional intensity space defined by FLAIR, T1-w, T2-w and Proton Density weighted images and trained on 11 manually annotated subjects;¹² 2) the patch-based Subject Specific Sparse Dictionary Learning (S3DL) method,¹⁹ which takes FLAIR and T1-weighted images as input for lesion segmentation as well as three manually annotated atlases; and 3) the whole brain segmentation method FreeSurfer,¹⁷ which only takes a T1-weighted image as input, but is included in the comparison due to its widespread use. For each of the methods above, the preprocessing steps were as described in their associated publications. A visual comparison of the methods is shown for two subjects in Figure 2. The top row in Figure 2 demonstrates that SegAE can accurately segment lesion boundaries of the test image with the largest lesion load. The bottom row shows an example of a subject with a smaller lesion load but with enlarged ventricles.

The Dice score, Positive Predictive Value (PPV), True Positive Rate (TPR), and Absolute Volume Difference (AVD) were used as quantitative evaluation metrics, as described in Carass et al.² Figure 3 shows box plots of AVD, Dice, PPV, and TPR scores for each method. The mean values and standard deviations are reported in Table 1. SegAE achieves the lowest average AVD of 0.255, the highest Dice score of 0.766 ($p < 0.005$), the highest average PPV of 0.757, and the highest average TPR of 0.802. The p-values from a paired Wilcoxon signed-rank test comparing the AVD, Dice, PPV, and TPR scores of SegAE to the Supervised method, FreeSurfer, and S3DL can be seen in Table 2. We compared the predicted lesion volumes to the manual lesion volumes in Figure 4. The solid lines show a linear fit of the points and the dashed black lines have a unit slope. We observe that the Supervised method systematically overestimates lesion volumes of both small and large lesions. FreeSurfer and S3DL seem to underestimate most lesion volumes in this data set. SegAE does not show such a bias, although the predicted volumes of the four largest lesions are slightly smaller than the manual volumes. Table 3 shows the slopes and intercepts of the linear fits between the five methods and the manual volumes.

4. CONCLUSIONS

We have presented SegAE, a convolutional autoencoder architecture that can be used for unsupervised segmentation of WM brain lesions from MRIs. We note that an important byproduct of the approach is a classification of the brain into WM, GM, and CSF (results not reported). The model was trained and evaluated on a data set

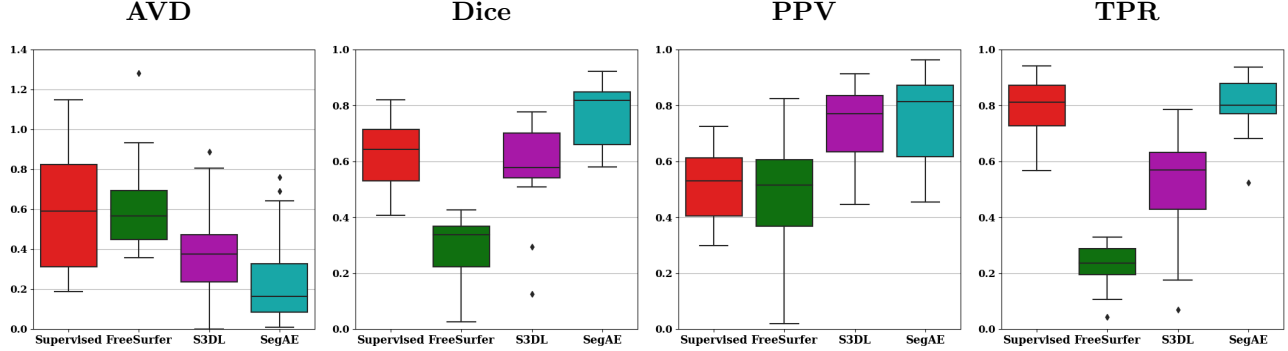


Figure 3. Boxplots showing the AVD, Dice, PPV, and TPR scores of Supervised (red), FreeSurfer (green), S3DL (magenta), and SegAE (cyan), respectively.

Table 1. The mean and standard deviation of Absolute Volume Difference (AVD), Dice, Positive Predictive Value (PPV), and True Positive Rate (TPR) for the proposed method SegAE, and three alternative methods. Asterisk (*) denotes that a value is significantly different ($p < 0.005$) from SegAE, and bold figures denote the best result.

	AVD	Dice	PPV	TPR
Supervised	0.605 (± 0.298)*	0.622 (± 0.127)*	0.517 (± 0.134)*	0.794 (± 0.107)
FreeSurfer	0.611 (± 0.238)*	0.294 (± 0.113)*	0.479 (± 0.224)*	0.226 (± 0.081)*
S3DL	0.370 (± 0.241)	0.571 (± 0.167)*	0.735 (± 0.144)	0.516 (± 0.193)*
SegAE	0.255 (± 0.240)	0.766 (± 0.114)	0.757 (± 0.169)	0.802 (± 0.099)

Table 2. The p-values of a paired Wilcoxon signed-rank test (without correction for multiple comparisons) comparing the AVD, Dice, PPV, and TPR scores of SegAE and the Supervised method, FreeSurfer, and S3DL.

	AVD	Dice	PPV	TPR
SegAE vs. Supervised	0.0008	0.0007	0.0007	0.6909
SegAE vs. FreeSurfer	0.0064	0.0007	0.0007	0.0007
SegAE vs. S3DL	0.1728	0.0007	0.0691	0.0007

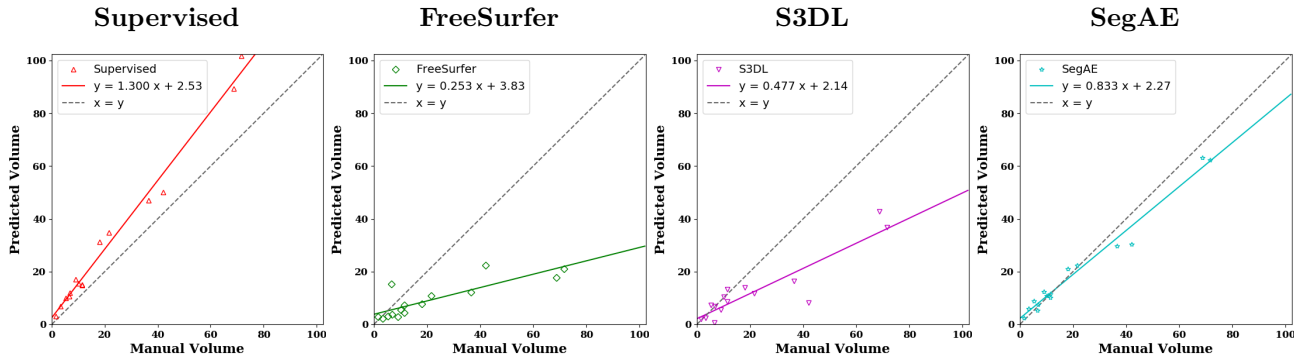


Figure 4. Predicted lesion volumes versus manual lesion volumes for the 4 methods. The solid lines show a linear fit of the points and the dashed black line has unit slope. Numbers are in cm^3 .

Table 3. Slopes and intercepts from Figure 4.

	Supervised	FreeSurfer	S3DL	SegAE
Slope	1.300	0.253	0.477	0.833
Intercept	2.533	3.828	2.144	2.273

with a high variability in lesion load. The lesion segmentation was evaluated on 15 manually labeled subjects and compared with three state-of-the-art tissue and lesion segmentation methods. SegAE achieves the lowest mean AVD, the highest Dice (significantly higher than all three methods, $p < 0.005$), the highest mean PPV, and the highest mean TPR on these test images. Table 2 shows the p-values comparing the three methods to SegAE.

Future work includes using a scale-invariant loss function to stabilize training, incorporating the other imaging modalities into the loss, exploring better methods of pre- and post-processing to prevent over-segmentation due to image artifacts, and a more extensive evaluation of the proposed method on a larger data set of manually delineated subjects.

5. ACKNOWLEDGEMENTS

This work was supported by RANNIS (The Icelandic Centre for Research) through grant 173942-051.

REFERENCES

- [1] Black, S., Gao, F., and Bilbao, J., “Understanding white matter disease: imaging-pathological correlations in vascular cognitive impairment,” *Stroke* **40**(3_suppl_1), S48–S52 (2009).
- [2] Carass, A., Roy, S., Jog, A., Cuzzocreo, J. L., Magrath, E., Gherman, A., Button, J., Nguyen, J., Prados, F., Sudre, C. H., et al., “Longitudinal multiple sclerosis lesion segmentation: resource and challenge,” *NeuroImage* **148**, 77–102 (2017).
- [3] Li, H., Jiang, G., Zhang, J., Wang, R., Wang, Z., Zheng, W.-S., and Menze, B., “Fully convolutional network ensembles for white matter hyperintensities segmentation in mr images,” *NeuroImage* **183**, 650–665 (2018).
- [4] Roy, S., Butman, J. A., Reich, D. S., Calabresi, P. A., and Pham, D. L., “Multiple sclerosis lesion segmentation from brain mri via fully convolutional neural networks,” *arXiv preprint arXiv:1803.09172* (2018).
- [5] Garcia-Lorenzo, D., Prima, S., Arnold, D. L., Collins, D. L., and Barillot, C., “Trimmed-likelihood estimation for focal lesions and tissue segmentation in multisequence mri for multiple sclerosis,” *IEEE Transactions on Medical Imaging* **30**(8), 1455–1467 (2011).
- [6] Schmidt, P., Gaser, C., Arsic, M., Buck, D., Förschler, A., Berthele, A., Hoshi, M., Ilg, R., Schmid, V. J., Zimmer, C., et al., “An automated tool for detection of flair-hyperintense white-matter lesions in multiple sclerosis,” *Neuroimage* **59**(4), 3774–3783 (2012).
- [7] Lladó, X., Oliver, A., Cabezas, M., Freixenet, J., Vilanova, J. C., Quiles, A., Valls, L., Ramió-Torrentà, L., and Rovira, À., “Segmentation of multiple sclerosis lesions in brain mri: a review of automated approaches,” *Information Sciences* **186**(1), 164–185 (2012).
- [8] Tomas-Fernandez, X. and Warfield, S. K., “A model of population and subject (mops) intensities with application to multiple sclerosis lesion segmentation,” *IEEE transactions on medical imaging* **34**(6), 1349–1361 (2015).
- [9] Bowles, C., Qin, C., Guerrero, R., Gunn, R., Hammers, A., Dickie, D. A., Hernández, M. V., Wardlaw, J., and Rueckert, D., “Brain lesion segmentation through image synthesis and outlier detection,” *NeuroImage: Clinical* **16**, 643–658 (2017).
- [10] Baur, C., Wiestler, B., Albarqouni, S., and Navab, N., “Deep autoencoding models for unsupervised anomaly segmentation in brain MR images,” *arXiv preprint arXiv:1804.04488* (2018).
- [11] Pawlowski, N., Lee, M. C., Rajchl, M., McDonagh, S., Ferrante, E., Kamnitsas, K., Cooke, S., Stevenson, S., Khetani, A., Newman, T., et al., “Unsupervised lesion detection in brain CT using bayesian convolutional autoencoders,” *MIDL Medical Imaging with Deep Learning, accessed from OpenReview.net* (2018).
- [12] Sigurdsson, S., Aspelund, T., Forsberg, L., Fredriksson, J., Kjartansson, O., Oskarsdottir, B., Jonsson, P. V., Eiriksdottir, G., Harris, T. B., Zijdenbos, A., et al., “Brain tissue volumes in the general population of the elderly: the ages-reykjavik study,” *Neuroimage* **59**(4), 3862–3870 (2012).
- [13] Tustison, N. J., Avants, B. B., Cook, P. A., Zheng, Y., Egan, A., Yushkevich, P. A., and Gee, J. C., “N4itk: improved n3 bias correction,” *IEEE transactions on medical imaging* **29**(6), 1310–1320 (2010).
- [14] Fonov, V. S., Evans, A. C., McKinstry, R. C., Almlí, C., and Collins, D., “Unbiased nonlinear average age-appropriate brain templates from birth to adulthood,” *NeuroImage* (47), S102 (2009).

- [15] Roy, S., Butman, J. A., and Pham, D. L., “Robust skull stripping using multiple MR image contrasts insensitive to pathology,” *Neuroimage* **146**, 132–147 (Feb 2017).
- [16] Palsson, B., Sigurdsson, J., Sveinsson, J. R., and Ulfarsson, M. O., “Hyperspectral unmixing using a neural network autoencoder,” *IEEE Access* **6**, 25646–25656 (2018).
- [17] Fischl, B., “Freesurfer,” *Neuroimage* **62**(2), 774–781 (2012).
- [18] Kingma, D. P. and Ba, J., “Adam: A method for stochastic optimization,” *arXiv preprint arXiv:1412.6980* (2014).
- [19] Roy, S., He, Q., Sweeney, E., Carass, A., Reich, D. S., Prince, J. L., and Pham, D. L., “Subject specific sparse dictionary learning for atlas based brain mri segmentation,” *IEEE journal of biomedical and health informatics* **19**(5), 1598 (2015).